

# A Mechanism-Based Antioxidant Approach for the Reduction of Skin Carcinogenesis

Yunfeng Zhao,<sup>1</sup> Luksana Chaiswing,<sup>3,5</sup> Terry D. Oberley,<sup>3,4</sup> Ines Batinic-Haberle,<sup>6</sup> William St. Clair,<sup>2</sup> Charles J. Epstein,<sup>7</sup> and Daret St. Clair<sup>1</sup>

<sup>1</sup>Graduate Center for Toxicology and <sup>2</sup>Department of Radiation Medicine, University of Kentucky, Lexington, Kentucky; <sup>3</sup>Department of Pathology and <sup>4</sup>Veterans Affairs Medical Center, University of Wisconsin, Madison, Wisconsin; <sup>5</sup>Faculty of Medical Technology, Mahidol University, Bangkok, Thailand; <sup>6</sup>Department of Radiation Oncology, Duke University, Durham, North Carolina; and <sup>7</sup>Department of Pediatrics, University of California, San Francisco, California

## Abstract

Studies in our laboratories showed that overexpression of manganese superoxide dismutase (MnSOD) reduced tumor incidence in a multistage skin carcinogenesis mouse model. However, reduction of MnSOD by heterozygous knockout of the *MnSOD* gene (MnSOD KO) did not lead to an increase in tumor incidence, because a reduction of MnSOD enhanced both cell proliferation and apoptosis. The present study extends our previous studies in the MnSOD KO mice and shows that apoptosis in mouse epidermis occurred prior to cell proliferation (6 versus 24 hours) when treated with tumor promoter 12-*O*-tetradecanoylphorbol-13-acetate (TPA). To investigate the possibility that a timed administration of SOD following apoptosis but before proliferation may lead to suppression of tumor incidence, we applied a SOD mimetic (MnTE-2-PyP<sup>5+</sup>) 12 hours after each TPA treatment. Biochemical studies showed that MnTE-2-PyP<sup>5+</sup> suppressed the level of protein carbonyls and reduced the activity of activator protein-1 and the level of proliferating cellular nuclear antigen, without reducing the activity of p53 or DNA fragmentation following TPA treatment. Histologic examination confirmed that MnTE-2-PyP<sup>5+</sup> suppressed mitosis without interfering with apoptosis. Remarkably, the incidence and multiplicity of skin tumors were reduced in mice that received MnTE-2-PyP<sup>5+</sup> before cell proliferation. These results show a novel strategy for an antioxidant approach to cancer intervention. (Cancer Res 2005; 65(4): 1401-5)

## Introduction

Manganese superoxide dismutase (MnSOD), a primary antioxidant enzyme localized in mitochondria (1), has been shown to act as a tumor suppressor and redox modulator. Increased expression of MnSOD has been shown to suppress cancer phenotypes in a large number of mammalian tumor cells (2–10) and in animal tumor models (10–12). To determine whether and how expression of MnSOD may suppress the development of cancer *in situ*, in our previous studies, we employed a well-established skin carcinogenesis model consisting of sequential application of a subthreshold dose of the mutagenic chemical initiator 7,12-dimethylbenz(*a*)-anthracene (DMBA), followed by repetitive treatments with the tumor promoter 12-*O*-tetradecanoylphorbol-13-acetate (TPA).

**Requests for reprints:** Daret St. Clair, Graduate Center for Toxicology, University of Kentucky, Lexington, KY. Phone: 859-257-3956; Fax: 859-323-1059; E-mail: dstcl00@pop.uky.edu.

©2005 American Association for Cancer Research.

In a MnSOD transgenic mice model, 78% of nontransgenic mice developed papillomas, averaging 2.1 papillomas per mouse, whereas 50% of MnSOD overexpressing mice developed papillomas, averaging 0.75 papillomas per mouse after 14 weeks of TPA treatment, following a single application of DMBA (12). These results suggested that MnSOD modulates tumor formation by inhibition of activator protein-1 (AP-1) signaling, resulting in reduction of tumors in MnSOD overexpressing mice. Surprisingly, in a MnSOD heterozygous knockout mouse model (MnSOD KO), there was no difference in the incidence and frequency of papillomas when comparing the MnSOD KO mice with their wild-type (WT) littermates (13). However, histologic examination showed that the number of proliferating cells in DMBA/TPA-treated mouse skin were higher in the KO mice. Histologic examination also showed a concurrent increase in the numbers of apoptotic cells in the KO mice after DMBA/TPA treatment. Furthermore, MnSOD deficiency enhanced TPA-induced oxidative stress markers, AP-1 and p53 levels, consistent with the increase in both proliferation and apoptosis events observed histologically in the MnSOD KO mice. Thus, increased apoptosis may negate the effect of increased proliferation in the MnSOD-deficient mice during an early stage of tumor development. Based upon these findings, we hypothesize that inhibiting proliferation without interfering with apoptosis could be an effective mean to prevent papilloma formation.

Herein, we did the timed administration of a SOD mimetic (MnTE-2-PyP<sup>5+</sup>) using the multistage skin carcinogenesis model in MnSOD KO mice to show a proof of this principle.

## Materials and Methods

**Mice.** Heterozygous DBA/2 MnSOD KO mice (*sod2*  $-/+$ ) were originally produced in the CD1 strain of mice (14). The WT DBA/2 mice were purchased from the Jackson Laboratory (Indianapolis, IN). Heterozygous mice have since been back-crossed to DBA/2 mice for >20 generations. The MnSOD activity in the skin of the KO mice was close to 50% of that in the wild type counterparts ( $23.0 \pm 1.9$  versus  $50.3 \pm 4.0$  units/mg, respectively). The activity was measured using the method described by Spitz and Oberley (15). For all experiments, 6- to 8-week-old female mice were used.

**SOD Mimetic.** MnTE-2-PyP<sup>5+</sup> was synthesized as previously described (16). The electrostatic facilitation of O<sub>2</sub><sup>-</sup> dismutation and favorable metal-centered redox potential (17) resulted in a high catalytic dismutation rate of  $5.8 \times 10^7$  (mol/L)<sup>-1</sup> s<sup>-1</sup>. It has thus been effective in rodent models of oxidative stress injuries (17).

**Multistage Skin Carcinogenesis.** Hair on the back of female mice was shaved 2 days before application of vehicle or carcinogen. Mice in the resting stage of the hair cycle were chosen for subsequent treatment. A single dose of 100 nmol DMBA (Sigma, St. Louis, MO) dissolved in DMSO was painted on each mouse. After 2 weeks, 4  $\mu$ g of TPA, also dissolved in DMSO, was applied 5 days per week to the same area for 14 weeks.

MnTE-2-PyP<sup>5+</sup>, dissolved in 0.05 mol/L phosphate buffer (pH 7.4) was applied 5 days per week for 14 weeks to the skin (5 ng/mouse), either 30 minutes before or 12 hours after each TPA treatment. The dose of MnTE-2-PyP<sup>5+</sup> was determined from a pilot study.

After euthanasia, skin from each mouse was removed and fixed in 4% neutral buffered formaldehyde for subsequent pathologic examination. After rinsing with PBS, tissues were dehydrated with graded ethanol and embedded in paraffin. Paraffin sections were cut at 4  $\mu$ m and mounted on glass slides. Tissue sections were analyzed in a blinded fashion by a pathologist (T.D.O.) to determine the number of papillomas.

#### Histologic Examination of the Kinetics of Apoptosis versus Mitosis.

Fifty-four mice (27 for each MnSOD WT and KO group) were used in this study. Mice were treated with either DMSO (control) or single application of 100 nmol/L DMBA followed 2 weeks later by a single application of 4  $\mu$ g TPA. Animals were euthanized and skin samples were collected at 0, 1, 3, 6, 12, 24, 36, and 48 hours ( $n = 3$  for each group). For histologic examination, the tissues were fixed with Karnovsky's fixative for 1 hour at room temperature and then rinsed in 0.1 mol/L Sorenson's phosphate buffer (pH 7.4) for 30 minutes. Following fixation in Caulfield's osmium tetroxide with sucrose for 30 minutes, the tissues were dehydrated in graded ethanol and embedded in epoxy resin. Thick sections of Epon-embedded skin tissues were mounted on glass slides and stained with toluidine blue. Apoptotic and mitotic cells were counted by light microscopy. Only interfollicular epidermis was counted. Five hundred cells were counted per mouse. The following morphologic features were used to identify apoptosis: cell shrinkage, chromatin condensation, and formation of cytoplasmic blebs and apoptotic bodies. All phases of mitosis were included in the analysis. Results from various time points were compared with control using ANOVA

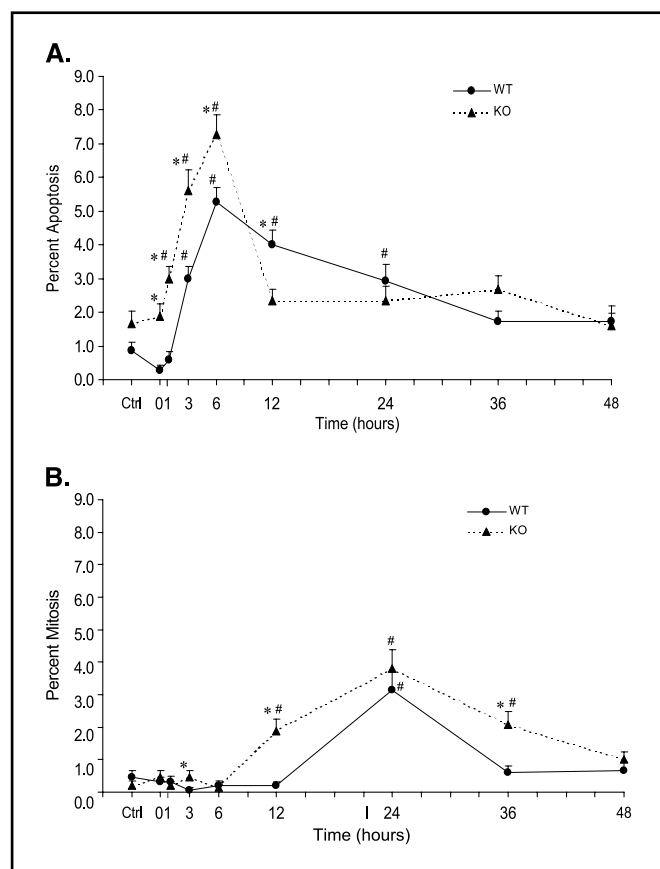


**Figure 1.** Kinetics of apoptosis and mitosis in mouse skin tissue. A, apoptosis; B, mitosis. Ctrl, vehicle control. \*,  $P < 0.05$ , significant difference for WT versus KO; #,  $P < 0.05$ , significant difference compared with the corresponding control group.

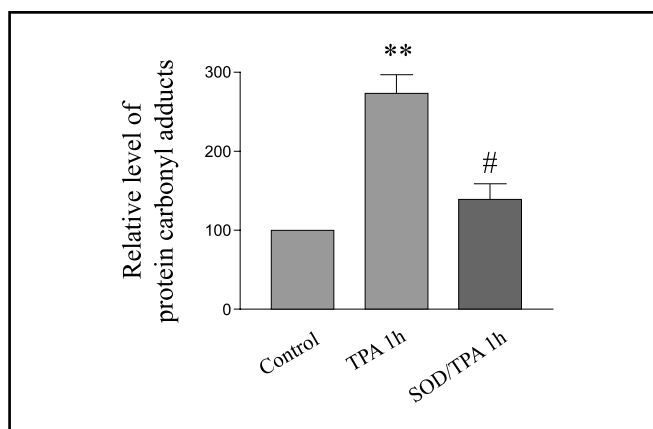


**Figure 2.** MnTE-2-PyP<sup>5+</sup> suppressed protein oxidation *in vivo*. Results were quantified from Western blots of protein carbonyl adducts. \*\*,  $P < 0.01$ , significant difference compared with the vehicle control group; #,  $P < 0.05$ , significant difference compared with the TPA group.

with LSD post hoc test. Statistical comparison between WT and KO mice at each time point was done with independent Student's  $t$  test.

For MnTE-2-PyP<sup>5+</sup> treatment, 12 MnSOD KO female mice were studied. Mice were treated with either DMSO (control,  $n = 3$ ); DMBA followed 2 weeks later with a single application of TPA ( $n = 3$ ); a single application of MnTE-2-PyP<sup>5+</sup> 30 minutes before TPA application ( $n = 3$ ) or 12 hours following TPA ( $n = 3$ ). In this group, 1,500 random keratinocytes were counted per mouse. Sample preparation and analysis procedures were identical to those described for the kinetics study.

**Preparation of Nuclear Extract from Skin Tissue.** Skin epidermal cells were stripped off and suspended in 800  $\mu$ L of buffer A (10 mmol/L HEPES-KOH with 1.5 mmol/L MgCl<sub>2</sub>, 10 mmol/L KCl, 0.2 mmol/L phenylmethylsulfonyl fluoride, 5  $\mu$ mol/L of DTT) containing protease inhibitors (5  $\mu$ g/mL each of pepstatin, leupeptin and aprotinin) and homogenized in a 10-mL Wheaton homogenizer. After a short spin, the supernatant was kept on ice for 30 minutes; 25  $\mu$ L of 10% NP40 was then added and the sample was vortexed vigorously for 25 seconds. The lysate was centrifuged at 14,000 rpm for 1 minute. The resulted pellet was dissolved in 120  $\mu$ L of buffer B [20 mmol/L HEPES-KOH with 1.5 mmol/L MgCl<sub>2</sub>, 420 mmol/L NaCl, 35% glycerol, 0.2 mmol/L phenylmethylsulfonyl fluoride, 5  $\mu$ M of DTT, 0.2 mmol/L EDTA (pH 8.0)] containing protease inhibitors. The sample was kept on ice for 30 minutes, centrifuged at 12,000 rpm for 5 minutes, and the supernatant, identified as *nuclear extract*, was frozen at  $-80^{\circ}\text{C}$ .

**Preparation of Cytosolic Fraction from Skin Tissue.** The cytosolic fraction was prepared as previously described (12, 13). Skin epidermal cells were stripped and extracted by homogenization in 1 mL of homogenization buffer [20 mmol/L HEPES (pH 7.0), 5 mmol/L EGTA, 10 mmol/L 2-mercaptoethanol, 1 mmol/L phenylmethylsulfonyl fluoride, and 1  $\mu$ g/mL each of protein inhibitors]. The lysate was centrifuged (50  $\times g$  or 600 rpm, 5 minutes) to remove tissue debris. The resulting supernatant was centrifuged at 10,000  $\times g$  for 1 hour at  $4^{\circ}\text{C}$ . The supernatant was transferred into a new tube and designated as *cytosolic fraction* and kept at  $-80^{\circ}\text{C}$ .

**Isolation of Mitochondrial Fraction from Skin Tissues.** Stripped skin epidermal cells were suspended in 1 mL mitochondrial isolation buffer [0.225 mol/L mannitol, 0.075 mol/L sucrose, 1 mmol/L EGTA (pH 7.4)] and homogenized using scale 2 of a Wheaton homogenizer for thrice of 30-second strokes. The tissue was removed by centrifugation at 576  $\times g$  (2,200 rpm) for 5 minutes. The supernatant was filtered through a nylon screen cloth (Small Parts, Inc., Miami Lakes, FL) and centrifuged at 9,000  $\times g$  (8,700 rpm) for 10 minutes. The pellet was washed by adding 0.5 mL of mitochondrial isolation buffer and centrifuging at 9,000  $\times g$  for 5 minutes. The pellet was resuspended in 150  $\mu$ L of mitochondrial isolation buffer containing 0.1% Triton X-100. This fraction was labeled the *mitochondrial fraction* and kept at  $-80^{\circ}\text{C}$ .

**Electrophoretic Mobility Shift Assays.** AP-1-DNA binding activity was analyzed in *nuclear extracts*. The AP-1 double-strand oligonucleotide (5'-CGCTTGATGAGTCAGCCGAA-3') was purchased from Promega (Madison, WI). A 25- $\mu$ L reaction solution contained 6  $\mu$ g of *nuclear extract*, 5  $\mu$ L of 5  $\times$  binding buffer [50 mmol/L Tris-HCl (pH 7.4), with 20% glycerol, 5 mmol/L MgCl<sub>2</sub>, 2.5 mmol/L EDTA, 5 mmol/L DTT, and 0.25 mg/mL poly dI-dC] and 50,000 cpm labeled probe. After 20 minutes of incubation, the samples were separated on a 6% native polyacrylamide gel. DNA-protein complexes were visualized by exposing the gels to Kodak film at  $-80^{\circ}\text{C}$ .

**Western Blot Analysis.** Protein concentration of the samples was measured by a colorimetric assay (Bio-Rad Laboratories, Richmond, CA). The *mitochondrial fraction* was used to detect p53 immunoreactive protein. Primary mouse antibody against p53 was purchased from Oncogene (Boston, MA).

The *nuclear extract* was used to detect nuclear proliferating cellular nuclear antigen (PCNA), the primary anti-PCNA antibody was purchased from Santa Cruz Biotechnology (Santa Cruz, CA). For detection of oxidatively modified proteins, the *cytosolic fraction* was used. The OxyBlot protein oxidation detection kit (s7150, Intergen, Purchase, NY) was chosen to perform the assay. The reaction procedures were done according to the manufacturer's instructions.

**DNA Fragmentation.** Cell Death Detection ELISA (Roche Molecular Biochemicals, Indianapolis, IN) was used to determine DNA fragmentation. One hundred  $\mu$ g of the *cytosolic fraction* was used for the assay. The experiments were done according to the manufacturer's instructions.

**Statistical Analysis.** Statistical analysis for biochemical studies was done using one-way ANOVA with Newman-Keuls following test. Data are reported as means  $\pm$  SD.

## Results

**Apoptosis Precedes Cell Proliferation.** In a previous study, we showed that TPA-induced oxidative stress and an increase in both apoptosis and proliferation in mouse skin epidermis. Herein, we did a detailed time course analysis of apoptosis and mitosis. Histologic examination showed that apoptotic and mitotic cells were found almost exclusively in the basal layer of the epidermis (data not shown). However, the kinetics of the two events was different. There was an early increase in apoptosis in interfollicular keratinocytes from both WT and KO mouse skin following treatment with TPA. In both types of mice, there was a peak of apoptosis at 6 hours, which was  $\sim$ 5-fold greater than controls in both WT and KO mice (Fig. 1). Apoptosis was present at 12, 24, 36, and 48 hours in both strains of mice, but levels were much lower than observed apoptosis peak at 6 hours.

An increase in mitosis was observed at later time points in both WT and KO mouse skin after TPA application. In both strains of mice, the peaks of mitosis occurred at 24 hours, a time at which apoptosis was much lower than observed peak at 6 hours. The peak mitosis rate was  $\sim$ 3-fold greater than control in both strains of mice. However, the percent mitosis was greater in KO than WT mice, with significant increases compared with

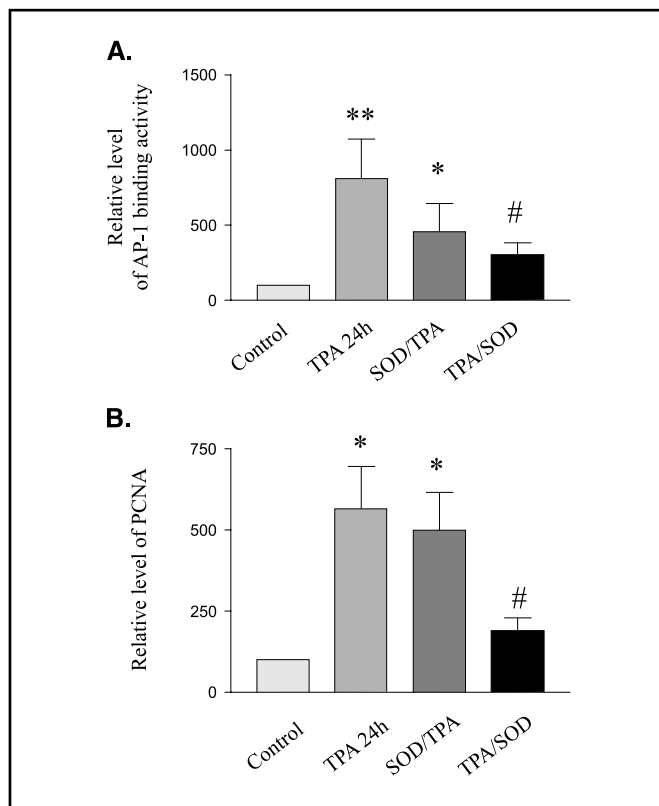


**Figure 3.** MnTE-2-PyP<sup>5+</sup> suppressed cell proliferation markers, AP-1 and PCNA. *A*, electrophoretic mobility shift assay detection of AP-1 binding activity. *B*, Western analysis of the levels of PCNA. \*,  $P < 0.05$ , significant difference from the vehicle control group; \*\*,  $P < 0.01$ , significant difference comparing with the vehicle control group; #,  $P < 0.05$ , significant difference compared with the TPA alone group.

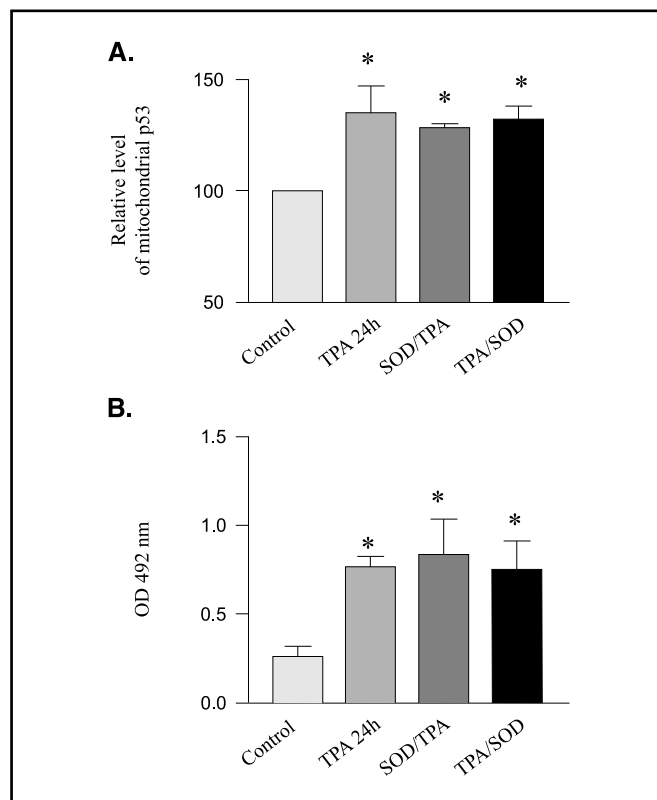


**Figure 4.** MnTE-2-PyP<sup>5+</sup> did not suppress markers associated with apoptosis. *A*, p53 protein levels in the mitochondria. *B*, DNA fragmentation detected by Cell Death ELISA. \*,  $P < 0.05$ , significant difference compared with the vehicle control group.

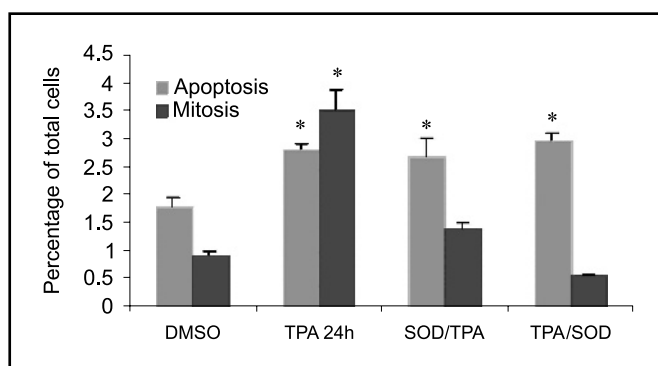


**Figure 5.** Light microscopic examination of mitosis and apoptosis. Data represent the means of four sets of independent experiments. \*,  $P < 0.05$ , significant difference compared with the vehicle control group.

control occurring at 3, 12, 24, and 36 hours in KO mice, but only at 24 hours in WT mice. Thus, 18 hours between the peaks of apoptosis and mitosis leaves a window of opportunity for an antioxidant therapeutic approach in order to suppress cell proliferation after apoptosis has occurred.

**Protein Oxidation in Skin Epidermal Cells.** It is well recognized that DMBA or TPA treatment can cause oxidative stress (18, 19). We have previously shown that TPA application induced rapid oxidative stress at the subcellular level as indicated by increased formation of carbonyl groups (aldehydes and ketones), a standard biomarker of oxidative damage, which are formed in the amino side chains of proteins (13). To verify the antioxidant potential of MnTE-2-PyP<sup>5+</sup>, whereas applied to mouse skin, we applied MnTE-2-PyP<sup>5+</sup> (5 ng/mouse) 30 minutes before TPA treatment, and protein carbonyl adducts were determined by Western blot. At 1 hour following TPA treatment, the levels of oxidatively modified proteins were significantly increased and MnTE-2-PyP<sup>5+</sup> significantly reduced the levels of protein carbonyl adducts. The result confirmed that MnTE-2-PyP<sup>5+</sup> suppressed oxidative stress induced by TPA in mouse skin (Fig. 2).

**Biochemical Markers of Cell Proliferation and Apoptosis.** TPA is known to cause an activation of AP-1 and activates expression of several genes required for cell proliferation in the skin (20). The AP-1 DNA-binding activity detected by electrophoretic mobility shift assays was significantly increased within 24 hours following TPA treatment after a single application of DMBA (Fig. 3A). Treatment with MnTE-2-PyP<sup>5+</sup> either at 30 minutes before TPA (SOD/TPA) or at 12 hours following TPA application (TPA/SOD) showed reduced AP-1 binding activity. However, the suppressive effect was significant only when MnTE-2-PyP<sup>5+</sup> was given 12 hours following TPA treatment.

Western analysis of PCNA, a well-recognized marker for cell proliferation, indicated that, consistent with AP-1 inhibition, the levels of PCNA was significantly suppressed only when MnTE-2-PyP<sup>5+</sup> was given 12 hours following TPA treatment (Fig. 3B).

Because our histologic examination showed that mouse tissues treated with DMBA/TPA showed frequent apoptosis and preceding mitosis, we analyzed biochemical markers for apoptosis, including the protein levels of mitochondrial p53 and DNA fragmentation in skin samples. Western analysis revealed increased levels of mitochondrial p53 after TPA treatment (Fig. 4A), and the increase in mitochondrial p53 was not inhibited in MnTE-2-PyP<sup>5+</sup>-treated mice. Consistent with the

levels of mitochondrial p53, DNA fragmentation, a hallmark of apoptosis, which was induced by TPA treatment at 24 hours, was not significantly changed by MnTE-2-PyP<sup>5+</sup> (Fig. 4B).

**MnTE-2-PyP<sup>5+</sup> Suppressed Cell Mitosis without an Effect on Apoptosis.** The numbers of apoptotic and mitotic cells as examined histologically were counted and analyzed (Fig. 5). To compare with all treatment groups, we counted 1500 random keratinocytes per mouse in stead of 500 cells per mouse (for the kinetics study). There was a significant increase in the number of apoptotic and mitotic cells in epidermal cells 24 hours after TPA treatment. When MnTE-2-PyP<sup>5+</sup> was applied 30 minutes before TPA treatment, epidermal cells had nearly 50% decrease in mitotic cells. When MnTE-2-PyP<sup>5+</sup> was applied 12 hours following TPA application, the number of mitotic cells was decreased by 85%. The number of apoptotic cells remained unchanged among all treatment groups.

**MnTE-2-PyP<sup>5+</sup> Reduced Tumorigenesis.** To investigate the ultimate effect of catalytic antioxidant on tumorigenesis, MnTE-2-PyP<sup>5+</sup> was applied daily either 30 minutes before (SOD/TPA) or 12 hours following TPA treatment (TPA/SOD). Pathologic results are summarized in Table 1.

There were no papillomas found in mice treated with vehicle alone. There were 31 papillomas in the DMBA/TPA-treated group. Pretreatment with MnTE-2-PyP<sup>5+</sup> reduced the total papillomas to 17. Significantly, application of MnTE-2-PyP<sup>5+</sup> after apoptosis reduced the total number of papillomas to 5. Thus, when applied after the peak of apoptosis, MnTE-2-PyP<sup>5+</sup> reduced papilloma formation ~6-fold in comparison with mice treated with DMBA/TPA.

## Discussion

Numerous studies using cultured cells suggested that MnSOD, a primary antioxidant enzyme, might function as a new type of tumor suppressor gene (2–10). Using the well-established multistage skin carcinogenesis model, we have shown that overexpression of MnSOD reduced tumor incidence and multiplicity, which is, in part, mediated by reducing oxidative stress and activities of AP-1 (12).

Furthermore, studies with MnSOD-deficient mice confirmed and extended our finding on the role of MnSOD in suppressing AP-1 activity and provided important insights into the delicate relationship between the role of MnSOD in proliferation and apoptosis in an early stage of tumor development (13). The results showed that although cell turnover is drastically altered in MnSOD KO mice following DMBA/TPA treatment, resultant tumor formation is not changed, suggesting a tight regulation of apoptosis and proliferation in the mouse skin. An important

**Table 1.** Papilloma formation in MnTE-2-PyP<sup>5+</sup>-treated mice in multiple-stage carcinogenesis model

Treatment	No. mice	Tumor incidence (%)	Papillomas per mouse	Total papillomas
DMBA/TPA	12	92	2.6 ± 1.8	31
SOD/TPA	11	73	1.5 ± 1.5	17
TPA/SOD	11	45	0.5 ± 0.5	5
DMSO	3	0	0	0

observation from histologic examination is that both cell proliferation and apoptosis in DMBA/TPA-treated mouse skin were higher in KO mice, indicating that epithelial cell turnover was higher following chemical treatment in the KO mice. Thus, it is not surprising that there was no difference in the incidence and frequency of papillomas in the MnSOD KO mice from those in the WT mice identically treated. These results show important roles of MnSOD in regulation of cell proliferation and cell death, which in turn, modulate subsequent tumor formation. The most important message from these results is that although, the SOD mimetic inhibits both apoptosis and proliferation induced by TPA; when applied after the peak of apoptosis and before the peak of proliferation, the SOD mimetic can inhibit TPA-induced proliferation without suppressing TPA-induced apoptosis.

Our kinetics studies showed that apoptosis occurred prior to proliferation after a single treatment of TPA. The number of apoptotic epidermal cells increased after 3 hours, reached a peak at 6 hours, and then decreased at 12 hours. Whereas the number of mitotic epidermal cells increased at 12 hours and reached a peak at 24 hours following TPA treatment. There is an 18-hour window between the peaks of the two events. These results suggest that there is a window between the two events induced by oxidative stress, which provide an opportunity to suppress only the proliferating event without interfering with apoptosis. In the current study, we started a SOD mimetic (MnTE-2-PyP<sup>5+</sup>) treatment at 12 hours, after the peak of apoptosis but before the peak of mitosis, to inhibit only cell proliferation. Biochemical and histologic studies showed that this approach significantly

suppressed cell proliferation without interfering with apoptosis, leading to a remarkable reduction of tumor formation (five papillomas) when comparing mice treated with DMBA/TPA alone (31 papillomas) or treated with MnTE-2-PyP<sup>5+</sup> before TPA application (17 papillomas).

Overall, our results show a critical role of antioxidant in regulating tumorigenesis. The window between apoptosis and proliferation provides an opportunity to suppress cell proliferation without interfering with apoptosis, leading to reduction of tumor formation. This novel antioxidant approach may have broad impact in other similar situations. Because oxidative stress is involved in the mode of action of radiation and many other cancer therapeutic agents, our results suggest that giving antioxidants several hours after the radiation therapy or chemotherapy to inhibit compensatory cell proliferation without suppressing the apoptosis induced by the radiation and chemotherapeutic drugs may enhance the outcome of cancer treatment.

## Acknowledgments

Received 9/20/2004; revised 11/8/2004; accepted 12/3/2004.

**Grant support:** NIH grant CA 73599, in part by resources and the use of facilities of the William S. Middleton Memorial Veterans Administration Hospital at Madison, WI, Thailand Research Fund under the Golden Jubilee Program (L. Chaiswing), and DOD CDMRP BC024326 and Aeolus/Incara Pharmaceuticals, RTP, NC (I. Batinic-Haberle).

The costs of publication of this article were defrayed in part by the payment of page charges. This article must therefore be hereby marked advertisement in accordance with 18 U.S.C. Section 1734 solely to indicate this fact.

We thank Dr. Irwin Fridovich at Duke University for his many insightful suggestions of this study and Jamie Swanlund for technical support.

## References

- Weisiger RA, Fridovich I. Mitochondrial superoxide simutase. Site of synthesis and intramitochondrial localization. *J Biol Chem* 1973;248:4793-6.
- Church SL, Grant JW, Ridnour LA, et al. Increased manganese superoxide dismutase expression suppresses the malignant phenotype of human melanoma cells. *Proc Natl Acad Sci U S A* 1993;90:3113-7.
- Safford SE, Oberley TD, Urano M, St. Clair DK. Suppression of fibrosarcoma metastasis by elevated expression of manganese superoxide dismutase. *Cancer Res* 1994;54:4261-5.
- Li JJ, Oberley LW, St. Clair DK, Ridnour LA, Oberley TD. Phenotypic changes induced in human breast cancer cells by overexpression of manganese-containing superoxide dismutase. *Oncogene* 1995;10:1989-2000.
- Yan T, Oberley LW, Zhong W, St. Clair DK. Manganese-containing superoxide dismutase over-expression causes phenotypic reversion in SV40-transformed human lung fibroblasts. *Cancer Res* 1996; 56:2864-71.
- Liu R, Oberley TD, Oberley LW. Transfection and expression of MnSOD cDNA decreases tumor malignancy of human oral squamous carcinoma SCC-25 cells. *Hum Gene Ther* 1997;8:585-95.
- Amstad PA, Liu H, Ichimiya M, Berezsky IK, Trump BF. Manganese superoxide dismutase expression inhibits soft agar growth in JB6 clone41 mouse epidermal cells. *Carcinogenesis* 1997;18:479-84.
- Zhong W, Oberley LW, Oberley TD, St. Clair DK. Suppression of the malignant phenotype of human glioma cells by overexpression of manganese superoxide dismutase. *Oncogene* 1997;14:481-90.
- Lam EW, Zwacka R, Seftor EA, et al. Effects of antioxidant enzyme overexpression on the invasive phenotype of hamster cheek pouch carcinoma cells. *Free Radic Biol Med* 1999;27:572-9.
- Darby Weydert CJ, Smith BB, Xu L, et al. Inhibition of oral cancer cell growth by adenovirus MnSOD plus BCNU treatment. *Free Radic Biol Med* 2003;34: 316-29.
- Li N, Oberley TD, Oberley LW, Zhong W. Over-expression of manganese superoxide dismutase in DU145 human prostate carcinoma cells has multiple effects on cell phenotype. *Prostate* 1998;35:221-33.
- Zhao Y, Xue Y, Oberley TD, et al. Overexpression of manganese superoxide dismutase suppresses tumor formation by modulation of activator protein-1 signaling in a multistage skin carcinogenesis model. *Cancer Res* 2001;61:6082-8.
- Zhao Y, Oberley TD, Chaiswing L, et al. Manganese superoxide dismutase deficiency enhances cell turnover via tumor promoter-induced alterations in AP-1 and p53-mediated pathways in a skin cancer model. *Oncogene* 2002;21:3836-46.
- Li Y, Huang TT, Carlson EJ, et al. Dilated cardiomyopathy and neonatal lethality in mutant mice lacking manganese superoxide dismutase. *Nat Genet* 1995;11:376-81.
- Spitz DR, Oberley LW. An assay for superoxide dismutase activity in mammalian tissue homogenates. *Anal Biochem* 1989;179:8-18.
- Batinic-Haberle I, Spasojevic I, Hambricht P, Benov L, Crumbliss AL, Fridovich I. Relationship among redox potentials, proton dissociation constants of pyrrolic nitrogens, and *in vivo* and *in vitro* superoxide dismuting activities of manganese(III) and iron(III) water-soluble porphyrins. *Inorg Chem* 1999;38:4011-22.
- Spasojevic I, Batinic-Haberle I, Reboucas JS, Idemori YM, Fridovich I. Electrostatic contribution in the catalysis of O<sub>2</sub><sup>-</sup>-dismutation by superoxide dismutase mimics. MnIIITE-2-PyP5+ versus MnIIIBr8T-2-PyP+. *J Biol Chem* 2003;278:6831-7.
- Khajuria A, Thusi N, Zutshi U, Bedi KL. Piperine modulation of carcinogen induced oxidative stress in intestinal mucosa. *Mol Cell Biochem* 1998;189: 113-8.
- Nakamura Y, Kawamoto N, Ohto Y, Torikai K, Murakami A, Ohgashi H. A diacetylenic spiroketal enol ether epoxide, AL-1, from *Artemisia lactiflora* inhibits 12-O-tetradecanoylphorbol-13-acetate-induced tumor promotion possibly by suppression of oxidative stress. *Cancer Lett* 1999;140:37-45.
- Bowden GT, Finch J, Domann F, Krieg P. Molecular mechanisms involved in skin tumor initiation, promotion and progression. In: Mukhtar H, editor. *Skin cancer: mechanisms and human relevance*. Boca Raton: CRC Press; 1995. p. 99-111.